Eur. Phys. J. D **33**, 59–65 (2005)
DOI: 10.1140/epjd/e2005-00036-6

THE EUROPEAN PHYSICAL JOURNAL D

Spherical nebulons and Bäcklund transformation for a space or laboratory un-magnetized dusty plasma with symbolic computation

Bo Tian[1,2] and Yi-Tian Gao[3,4,2]

[1] School of Science, P.O. Box 122, Beijing University of Posts and Telecommunications, Beijing 100876, China
[2] State Key Laboratory of Software Development Environment, Beijing University of Aeronautics and Astronautics, Beijing 100083, China
[3] CCAST (World Lab.), P.O. Box 8730, Beijing 100080, China
[4] Ministry-of-Education Key Laboratory of Fluid Mechanics and National Laboratory for Computational Fluid Dynamics, Beijing University of Aeronautics and Astronautics, Beijing 100083, China[a]

Received 25 January 2005 / Received in final form 18 February 2005
Published online 11 April 2005 – © EDP Sciences, Società Italiana di Fisica, Springer-Verlag 2005

Abstract. Plasmas and dust are a couple of the ubiquitous elements of the Universe. The nonlinear dust-acoustic-wave propagation in a space or laboratory un-magnetized dusty plasma is hereby considered, which is described by a spherical Kadomtsev-Petviashvili equation. By virtue of computerized symbolic computation, we obtain the analytically-expressed spherical nebulons and an auto-Bäcklund transformation for the electrostatic potential in such a plasma. With figures, we discuss the features of the nebulon structures, and propose some (3+1)-dimensional, possibly-observable nebulonic effects for the future space/laboratory plasma experiments.

PACS. 52.35.Mw Nonlinear phenomena: waves, wave propagation, and other interactions (including parametric effects, mode coupling, ponderomotive effects, etc.) – 52.35.Sb Solitons; BGK modes – 52.35.Fp Electrostatic waves and oscillations (e.g., ion-acoustic waves) – 02.70.Wz Symbolic computation (computer algebra) – 05.45.Yv Solitons

1 Introduction

The word "nebulon" presented in this paper comes after the astrophysical word "nebula", or the cloudlike structure observed in the Milky Way, which is composed of dust and gas, as stated, e.g., in references [1]. Specifically speaking, the nebulon structures as shown in Figures 2 and 6 via solution (24) in this paper look like the gaseous shell of the Ring nebula in Lyra, as seen in Figure 1, the photograph given by reference [2]. The nebulon structures are solitonic, and can exist beyond the normal solitary or travelling waves.

Plasmas and charged dust are a couple of the omnipresent components of the Universe. They are seen everywhere, such as in the tokamaks, microelectronic processing devices, planetary rings, cometary comae and tails, interstellar molecular clouds, noctilucent clouds in the arctic troposphere and mesosphere, lightening in thunderstorms, etc. The plasma instruments of spacecrafts

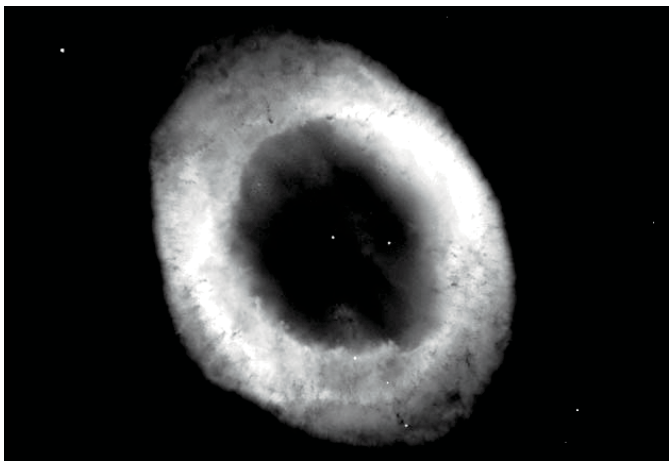

Fig. 1. Ring nebula (M57), about one light-year across and 2,000 light-years away in the northern constellation Lyra. Photograph credit: reference [2].

[a] Mailing address for YTG: gaoyt@public.bta.net.cn

Voyager 1, Voyager 2 and ICE have detected small dust particles striking them [3]. See, e.g., reference [4] and references therein for a brief review.

For the space and laboratory un-magnetized dusty plasmas, people have well understood the linear properties of the dust acoustic waves [5,6], in which the inertia comes from the dust-particle mass with the restoring force from the pressures of inertialess electrons and ions, and have turned the attention towards the nonlinear properties there [7–9]. A good example is the systematic, planar-geometry efforts on the dust acoustic solitary waves [5,8,10], although that geometry may not be realistic for the space and laboratory devices [11,12]. The observed features in the auroral region cannot be accounted for by a purely planar-geometry model [13], and the recent theoretical results with the nonplanar geometry also differ a lot from the planar ones [11,12,14].

Reference [11] focuses on the spherical dust acoustic solitary waves in an un-magnetized dusty plasma whose constituents are negatively-charged cold dust fluid and Boltzmann electrons and ions. Reference [12] generalizes such work by studying the transverse perturbation with the wave propagating in an axle-symmetry spherical geometry. The nonlinear dynamics of low phase speed (in comparison with the electron and ion thermal speeds) dust acoustic waves is governed [11,12] by

$$\frac{\partial n_d}{\partial t} + \frac{1}{r^2}\,\frac{\partial\left(r^2\, n_d\, u_d\right)}{\partial r} + \frac{1}{r}\,\frac{\partial\left(n_d\, u_d\right)}{\partial\theta} + \frac{n_d\, v_d}{r}\cot\theta = 0, \tag{1}$$

$$\frac{\partial u_d}{\partial t} + u_d\,\frac{\partial u_d}{\partial r} + \frac{v_d}{r}\,\frac{\partial u_d}{\partial\theta} - \frac{v_d^2}{r} = \frac{\partial\Phi}{\partial r}, \tag{2}$$

$$\frac{\partial v_d}{\partial t} + u_d\,\frac{\partial v_d}{\partial r} + \frac{v_d}{r}\,\frac{\partial v_d}{\partial\theta} + \frac{u_d\, v_d}{r} = \frac{1}{r}\,\frac{\partial\Phi}{\partial\theta}, \tag{3}$$

$$\frac{1}{r^2}\,\frac{\partial}{\partial r}\left(r^2\,\frac{\partial\Phi}{\partial r}\right) + \frac{1}{r^2}\,\frac{\partial^2\Phi}{\partial\theta^2} + \frac{\cot\theta}{r^2}\,\frac{\partial\Phi}{\partial\theta} = n_d + \mu_e\, e^{\,\sigma_i\,\Phi} - \mu_i\, e^{-\Phi}, \tag{4}$$

where n_d is the dust particle number density normalized by its equilibrium value n_{d0}, t, r and θ are the time, radial and latitude coordinates under the axle symmetry with t and r in units of the dust plasma period $\omega_{p_d}^{-1} = \sqrt{m_d/4\,\pi\, n_{d0}\, Z_{d0}^2\, e^2}$ and Debye length $\lambda_{Dm} = \sqrt{k_B\, T_i/4\,\pi\, n_{d0}\, Z_{d0}\, e^2}$, u_d and v_d are the dust fluid velocities in r and θ directions normalized by the effective dust acoustic velocity $C_d = \sqrt{Z_{d0}\, k_B\, T_i/m_d}$, Φ is the electrostatic wave potential normalized by $k_B\, T_i/e$, $\sigma_i = T_i/T_e$, $\mu_e = n_{e0}/Z_{d0}\, n_{d0} = 1/(\mu-1)$ and $\mu_i = n_{i0}/Z_{d0}\, n_{d0} = \mu/(\mu-1)$ with $\mu = n_{i0}/n_{e0}$. From the set of equations (1–4) and by using the reductive perturbation technique, references [11,12] have introduced the stretched coordinates [14] as $\xi = \epsilon^{1/2}(r - v_0\, t)$, $\eta = \epsilon^{-1/2}\,\theta$ and $\tau = \epsilon^{3/2}\, t$, and expanded n_d, u_d, v_d and Φ in power series of a small parameter ϵ, e.g., $\Phi = \epsilon\,\Phi^{(1)} + \epsilon^2\,\Phi^{(2)} + \cdots$, so as to end up with the following spherical Kadomtsev-Petviashvili equation,

$$\left(\Phi_\tau + A\,\Phi\,\Phi_\xi + B\,\Phi_{\xi\xi\xi} + \frac{\Phi}{\tau}\right)_\xi + \frac{1}{2\,\tau^2\, v_0}\left(\frac{\Phi_\eta}{\eta} + \Phi_{\eta\eta}\right) = 0, \tag{5}$$

and some solitary wave solutions (mostly numerically), where $\Phi \equiv \Phi^{(1)}$, $B = v_0^3/2$ with the wave velocity as $v_0 = \pm(\mu_i + \mu_e\,\sigma_i)^{-1/2}$ (so that the waves propagate either outward or inward), and $A = -(1/2)\left[3/v_0 + v_0^3(\mu_e\,\sigma_i^2 - \mu_i)\right]$. Equation (5) has recently been derived out for the dust ion-acoustic waves [29]. In reference [11], equation (5) reduces to a modified Korteweg-de Vries equation, without the transverse perturbation. Other topics on the Kadomtsev-Petviashvili-typed equations can be found, e.g., in references [15,16].

In this paper, we will symbolically work out certain analytically-expressed nebulon structures and Bäcklund transformation to equation (5), and propose possibly observable effects for the future space and laboratory experiments.

2 Computerized symbolic computation and auto-Bäcklund transformation for the electrostatic potential in a space or laboratory un-magnetized dusty plasma

We will consider the general case of $A \neq 0$ and $v_0 \neq 0$ (or equivalently $B \neq 0$), as indicated via the definitions of those parameters, and perform symbolic computation with the truncated Painlevé expansion of the dependent variable in a Laurent series about the pole manifold $\psi(\xi,\eta,\tau) = 0$ in the sense of references [15,17,18]:

$$\Phi(\xi,\eta,\tau) = \psi^{-J}(\xi,\eta,\tau)\sum_{l=0}^{J}\Phi_l(\xi,\eta,\tau)\,\psi^l(\xi,\eta,\tau), \tag{6}$$

where $\Phi_l(\xi,\eta,\tau)$'s and $\psi(\xi,\eta,\tau)$ are all analytic functions with $\Phi_0(\xi,\eta,\tau) \neq 0$ and $\psi_\xi(\xi,\eta,\tau) \neq 0$, while J is the natural number determined via the leading-order analysis as $J = 2$, so that

$$\Phi(\xi,\eta,\tau) = \frac{\Phi_0(\xi,\eta,\tau)}{\psi(\xi,\eta,\tau)^2} + \frac{\Phi_1(\xi,\eta,\tau)}{\psi(\xi,\eta,\tau)} + \Phi_2(\xi,\eta,\tau). \tag{7}$$

$$\frac{\Phi_{0,\eta}}{2\,\eta\,\tau^2\,v_0\,\psi^2}+\frac{\Phi_{1,\eta}}{2\,\eta\,\tau^2\,v_0\,\psi}+\frac{\Phi_{2,\eta}}{2\,\eta\,\tau^2\,v_0}-\frac{\Phi_0\,\psi_\eta}{\eta\,\tau^2\,v_0\,\psi^3}-\frac{\Phi_1\,\psi_\eta}{2\,\eta\,\tau^2\,v_0\,\psi^2}-\frac{2\,\Phi_{0,\eta}\,\psi_\eta}{\tau^2\,v_0\,\psi^3}-\frac{\Phi_{1,\eta}\,\psi_\eta}{\tau^2\,v_0\,\psi^2}+\frac{3\,\Phi_0\,{\psi_\eta}^2}{\tau^2\,v_0\,\psi^4}+\frac{\Phi_1\,{\psi_\eta}^2}{\tau^2\,v_0\,\psi^3}+\frac{\Phi_{0,\eta\eta}}{2\,\tau^2\,v_0\,\psi^2}$$
$$+\frac{\Phi_{1,\eta\eta}}{2\,\tau^2\,v_0\,\psi}+\frac{\Phi_{2,\eta\eta}}{2\,\tau^2\,v_0}-\frac{\Phi_0\,\psi_{\eta\eta}}{\tau^2\,v_0\,\psi^3}-\frac{\Phi_1\,\psi_{\eta\eta}}{2\,\tau^2\,v_0\,\psi^2}+\frac{\Phi_{0,\xi}}{\tau\,\psi^2}-\frac{2\,\psi_\tau\,\Phi_{0,\xi}}{\psi^3}+\frac{A\,{\Phi_{0,\xi}}^2}{\psi^4}+\frac{\Phi_{1,\xi}}{\tau\,\psi}-\frac{\psi_\tau\,\Phi_{1,\xi}}{\psi^2}+\frac{2\,A\,\Phi_{0,\xi}\,\Phi_{1,\xi}}{\psi^3}+\frac{A\,{\Phi_{1,\xi}}^2}{\psi^2}+\frac{\Phi_{2,\xi}}{\tau}$$
$$+\frac{2\,A\,\Phi_{0,\xi}\,\Phi_{2,\xi}}{\psi^2}+\frac{2\,A\,\Phi_{1,\xi}\,\Phi_{2,\xi}}{\psi}+A\,{\Phi_{2,\xi}}^2-\frac{2\,\Phi_0\,\psi_\xi}{\tau\,\psi^3}-\frac{\Phi_1\,\psi_\xi}{\tau\,\psi^2}-\frac{2\,\Phi_{0,\tau}\,\psi_\xi}{\psi^3}-\frac{\Phi_{1,\tau}\,\psi_\xi}{\psi^2}+\frac{6\,\Phi_0\,\psi_\tau\,\psi_\xi}{\psi^4}+\frac{2\,\Phi_1\,\psi_\tau\,\psi_\xi}{\psi^3}-\frac{8\,A\,\Phi_0\,\Phi_{0,\xi}\,\psi_\xi}{\psi^5}$$
$$-\frac{6\,A\,\Phi_1\,\Phi_{0,\xi}\,\psi_\xi}{\psi^4}-\frac{4\,A\,\Phi_2\,\Phi_{0,\xi}\,\psi_\xi}{\psi^3}-\frac{6\,A\,\Phi_0\,\Phi_{1,\xi}\,\psi_\xi}{\psi^4}-\frac{4\,A\,\Phi_1\,\Phi_{1,\xi}\,\psi_\xi}{\psi^3}-\frac{2\,A\,\Phi_2\,\Phi_{1,\xi}\,\psi_\xi}{\psi^2}-\frac{4\,A\,\Phi_0\,\Phi_{2,\xi}\,\psi_\xi}{\psi^3}-\frac{2\,A\,\Phi_1\,\Phi_{2,\xi}\,\psi_\xi}{\psi^2}$$
$$+\frac{10\,A\,{\Phi_0}^2\,{\psi_\xi}^2}{\psi^6}+\frac{12\,A\,\Phi_0\,\Phi_1\,{\psi_\xi}^2}{\psi^5}+\frac{3\,A\,{\Phi_1}^2\,{\psi_\xi}^2}{\psi^4}+\frac{6\,A\,\Phi_0\,\Phi_2\,{\psi_\xi}^2}{\psi^4}+\frac{2\,A\,\Phi_1\,\Phi_2\,{\psi_\xi}^2}{\psi^3}-\frac{96\,B\,\Phi_{0,\xi}\,{\psi_\xi}^3}{\psi^5}-\frac{24\,B\,\Phi_{1,\xi}\,{\psi_\xi}^3}{\psi^4}$$
$$+\frac{120\,B\,\Phi_0\,{\psi_\xi}^4}{\psi^6}+\frac{24\,B\,\Phi_1\,{\psi_\xi}^4}{\psi^5}+\frac{\Phi_{0,\xi\tau}}{\psi^2}+\frac{\Phi_{1,\xi\tau}}{\psi}+\Phi_{2,\xi\tau}-\frac{2\,\Phi_0\,\psi_{\xi\tau}}{\psi^3}-\frac{\Phi_1\,\psi_{\xi\tau}}{\psi^2}+\frac{A\,\Phi_0\,\Phi_{0,\xi\xi}}{\psi^4}+\frac{A\,\Phi_1\,\Phi_{0,\xi\xi}}{\psi^3}+\frac{A\,\Phi_2\,\Phi_{0,\xi\xi}}{\psi^2}$$
$$+\frac{36\,B\,{\psi_\xi}^2\,\Phi_{0,\xi\xi}}{\psi^4}+\frac{A\,\Phi_0\,\Phi_{1,\xi\xi}}{\psi^3}+\frac{A\,\Phi_1\,\Phi_{1,\xi\xi}}{\psi^2}+\frac{A\,\Phi_2\,\Phi_{1,\xi\xi}}{\psi}+\frac{12\,B\,{\psi_\xi}^2\,\Phi_{1,\xi\xi}}{\psi^3}+A\,\Phi_2\,\Phi_{2,\xi\xi}+\frac{A\,\Phi_0\,\Phi_{2,\xi\xi}}{\psi^2}+\frac{A\,\Phi_1\,\Phi_{2,\xi\xi}}{\psi}$$
$$-\frac{2\,A\,{\Phi_0}^2\,\psi_{\xi\xi}}{\psi^5}-\frac{3\,A\,\Phi_0\,\Phi_1\,\psi_{\xi\xi}}{\psi^4}-\frac{A\,{\Phi_1}^2\,\psi_{\xi\xi}}{\psi^3}-\frac{2\,A\,\Phi_0\,\Phi_2\,\psi_{\xi\xi}}{\psi^3}-\frac{A\,\Phi_1\,\Phi_2\,\psi_{\xi\xi}}{\psi^2}+\frac{72\,B\,\Phi_{0,\xi}\,\psi_\xi\,\psi_{\xi\xi}}{\psi^4}+\frac{24\,B\,\Phi_{1,\xi}\,\psi_\xi\,\psi_{\xi\xi}}{\psi^3}$$
$$-\frac{144\,B\,\Phi_0\,{\psi_\xi}^2\,\psi_{\xi\xi}}{\psi^5}-\frac{36\,B\,\Phi_1\,{\psi_\xi}^2\,\psi_{\xi\xi}}{\psi^4}-\frac{12\,B\,\Phi_{0,\xi\xi}\,\psi_{\xi\xi}}{\psi^3}-\frac{6\,B\,\Phi_{1,\xi\xi}\,\psi_{\xi\xi}}{\psi^2}+\frac{18\,B\,\Phi_0\,{\psi_{\xi\xi}}^2}{\psi^4}+\frac{6\,B\,\Phi_1\,{\psi_{\xi\xi}}^2}{\psi^3}-\frac{8\,B\,\psi_\xi\,\Phi_{0,\xi\xi\xi}}{\psi^3}$$
$$-\frac{4\,B\,\psi_\xi\,\Phi_{1,\xi\xi\xi}}{\psi^2}-\frac{8\,B\,\Phi_{0,\xi}\,\psi_{\xi\xi\xi}}{\psi^3}-\frac{4\,B\,\Phi_{1,\xi}\,\psi_{\xi\xi\xi}}{\psi^2}+\frac{24\,B\,\Phi_0\,\psi_\xi\,\psi_{\xi\xi\xi}}{\psi^4}+\frac{8\,B\,\Phi_1\,\psi_\xi\,\psi_{\xi\xi\xi}}{\psi^3}$$
$$+\frac{B\,\Phi_{0,\xi\xi\xi\xi}}{\psi^2}+\frac{B\,\Phi_{1,\xi\xi\xi\xi}}{\psi}+B\,\Phi_{2,\xi\xi\xi\xi}-\frac{2\,B\,\Phi_0\,\psi_{\xi\xi\xi\xi}}{\psi^3}-\frac{B\,\Phi_1\,\psi_{\xi\xi\xi\xi}}{\psi^2}=0, \tag{8}$$

Substituting expression (7) into equation (5) with symbolic computation yields

see equation (8) above,

in which we make the coefficients of like powers of ψ to vanish, and obtain the Painlevé-Bäcklund equations as follows,

$$\psi^{-6}\text{:}\quad \Phi_0=-\frac{12\,B\,{\psi_\xi}^2}{A}, \tag{9}$$

$$\psi^{-5}\text{:}\quad \Phi_1=\frac{12\,B\,\psi_{\xi\xi}}{A}, \tag{10}$$

$$\psi^{-4}\text{:}\quad \mathcal{R}={\psi_\eta}^2+2\,\tau^2\,v_0\,\psi_\tau\,\psi_\xi+2\,A\,\tau^2\,v_0\,\Phi_2\,{\psi_\xi}^2 -6\,B\,\tau^2\,v_0\,{\psi_{\xi\xi}}^2+8\,B\,\tau^2\,v_0\,\psi_\xi\,\psi_{\xi\xi\xi}=0, \tag{11}$$

$$\psi^{-3}\text{:}\quad \frac{\mathcal{T}}{8}+\frac{9}{4}\,\eta\,\mathcal{R}_\xi\,\psi_\xi+\frac{9}{8}\,\eta\,\mathcal{R}\,\psi_{\xi\xi}\equiv 0 \qquad \text{where}$$
$$\mathcal{T}=8\,\psi_\eta\,{\psi_\xi}^2+8\,\eta\,\psi_{\eta\eta}\,{\psi_\xi}^2+16\,\eta\,\tau\,v_0\,{\psi_\xi}^3 -4\,A\,\eta\,\tau^2\,v_0\,{\psi_\xi}^3\,\Phi_{2,\xi}+12\,\eta\,\tau^2\,v_0\,{\psi_\xi}^2\,\psi_{\xi\tau}$$
$$-4\,\eta\,\psi_\eta\,\psi_\xi\,\psi_{\xi\eta}-\eta\,{\psi_\eta}^2\,\psi_{\xi\xi} -6\,\eta\,\tau^2\,v_0\,\psi_\tau\,\psi_\xi\,\psi_{\xi\xi}+6\,A\,\eta\,\tau^2\,v_0\,\Phi_2\,{\psi_\xi}^2\,\psi_{\xi\xi}$$
$$+6\,B\,\eta\,\tau^2\,v_0\,{\psi_{\xi\xi}}^3=0, \tag{12}$$

$$\psi^{-2}\text{:}\quad \mathcal{S}+\frac{3}{2}\,\eta\,\mathcal{R}_{\xi\xi}+\mathcal{Q}_\xi\,\psi_\xi\equiv 0 \qquad \text{where}$$
$$\mathcal{S}=\psi_\xi\,\psi_{\xi\eta}-\eta\,{\psi_{\xi\eta}}^2+\eta\,\psi_\xi\,\psi_{\xi\eta\eta} -2\,\eta\,\tau\,v_0\,\psi_\xi\,\psi_{\xi\eta\eta}-2\,\eta\,\tau^2\,v_0\,\psi_\xi\,\psi_{\xi\eta\eta}$$
$$-2\,B\,\eta\,\tau^2\,v_0\,\psi_\xi\,\psi_{\xi\eta\eta}+\psi_\eta\,\psi_{\xi\xi} +\eta\,\psi_{\eta\eta}\,\psi_{\xi\xi}+6\,\eta\,\tau\,v_0\,\psi_\xi\,\psi_{\xi\xi}$$
$$-2\,A\,\eta\,\tau^2\,v_0\,\psi_\xi\,\Phi_{2,\xi}\,\psi_{\xi\xi}-A\,\eta\,\tau^2\,v_0\,{\psi_\xi}^2\,\Phi_{2,\xi\xi} +3\,\eta\,\tau^2\,v_0\,\psi_\xi\,\psi_{\xi\xi\tau}-\eta\,\psi_\eta\,\psi_{\xi\xi\eta}$$
$$-\eta\,\tau^2\,v_0\,\psi_\tau\,\psi_{\xi\xi\xi}+2\,B\,\eta\,\tau^2\,v_0\,{\psi_{\xi\xi\xi}}^2=0, \tag{13}$$

ψ^{-1}: After twice of integration with respect to ξ,

$$\mathcal{Q}=\psi_\eta+2\,B\,\eta\,\tau^2\,v_0\,\psi_{\eta\eta} +\eta\,\left(1+2\,\tau\,v_0+2\,\tau^2\,v_0\right)\,\psi_{\eta\eta} +2\,A\,\eta\,\tau^2\,v_0\,\Phi_2\,\psi_{\xi\xi}=0, \tag{14}$$

$$\psi^0\text{:}\quad \left(\Phi_{2,\tau}+A\,\Phi_2\,\Phi_{2,\xi}+B\,\Phi_{2,\xi\xi\xi}+\frac{\Phi_2}{\tau}\right)_\xi +\frac{1}{2\,\tau^2\,v_0}\left(\frac{\Phi_{2,\eta}}{\eta}+\Phi_{2,\eta\eta}\right)=0. \tag{15}$$

What we have obtained is the set of equations (7) and (9–15), which constitutes an *auto-Bäcklund transformation* for the electrostatic potential in a space or laboratory unmagnetized dusty plasma, since the whole set is mutually consistent, or, explicitly solvable with respect to $\psi(\xi,\eta,\tau)$, $\Phi_0(\xi,\eta,\tau)$, $\Phi_1(\xi,\eta,\tau)$ and $\Phi_2(\xi,\eta,\tau)$, with a solved example seen next.

3 More comments on the Bäcklund transformations and related topics with symbolic computation

Symbolic computation is a new branch of artificial intelligence, with its remarkable feature as the permeation of computer sciences among various fields of science and engineering. Symbolic computation drastically increases the ability of a computer to exactly and algorithmically deal with the expressions, so that it is thought as the sign of modern scientific computations. Today, a new symbolic-computation-based research direction has been formed worldwide, to analytically investigate the solitonic phenomena and relevant nonlinear evolution equations which describe the underlying mechanisms of space plasmas, atmospheric and oceanic fluid dynamics, optical fiber communications, physics, chemistry, applied mathematics, biology, material sciences, etc. See references [16,19–21] for a review.

An auto-Bäcklund transformation works as a system of equations relating a "seed" solution of a nonlinear evolution equation to another (more complicated) solution of the same equation. This way, we would, in principle at least, be able to progressively construct more and more complicated solutions of the equation. For example, if the seed is a nebulon structure via solution (24) for the electrostatic potential in a space or laboratory un-magnetized dusty plasma, we could in principle construct a nebulonic "spectrum" for the electrostatic potential.

Beyond dusty plasmas, we have seen that the Bäcklund transformations can be applied to the investigations on the liquid surface waves in the presence of sea ice or surface tension [20], various water waves models [17,22–24], electron beam plasmas [25], elastic rod immersed inside a viscoelastic medium [26], etc. More comments on the Bäcklund transformations can be referred to, e.g., reference [27].

Of special interest, many recent symbolic-computation contributions have been summarized in a learned Princeton-Manhattan-Paderborn-Maplesoft review article [19].

4 Nebulons for the electrostatic wave potential

For the nebulonic features, we will construct a set of trial solutions,

$$\psi(\xi,\eta,\tau) = 1 + e^{\,\xi\,\alpha(\eta,\tau)+\beta(\eta,\tau)} \quad \text{and} \quad \Phi_2(\xi,\eta,\tau) = \sum_{n=0}^{\infty} \Phi_{2n}(\eta,\tau)\,\xi^n, \tag{16}$$

where the functions $\alpha(\eta,\tau)$, $\beta(\eta,\tau)$ and $\Phi_{2n}(\eta,\tau)$'s are sufficiently differentiable, with $\alpha \neq 0$ since $\psi_\xi \neq 0$. The ξ-linear and ξ-expansion forms are used solely for the simplification of the computation work. Using expressions (16) in the auto-Bäcklund transformation above, we perform symbolic computation, and get

$$\psi^{-4}\ \&\ \xi^n\text{:}\ \ \Phi_{2n} = 0 \qquad \text{for} \qquad n \geq 3, \tag{17}$$

$$\psi^{-4}\ \&\ \xi^2\text{:}\ \ \Phi_{22} = -\frac{{\alpha_\eta}^2}{2\,A\,\tau^2\,v_0\,\alpha^2}, \tag{18}$$

$$\psi^{-4}\ \&\ \xi^1\text{:}\ \ \Phi_{21} = -\frac{\tau^2\,v_0\,\alpha\,\alpha_\tau + \alpha_\eta\,\beta_\eta}{A\,\tau^2\,v_0\,\alpha^2}, \tag{19}$$

$$\psi^{-4}\ \&\ \xi^0\text{:}\ \ \Phi_{20} = -\frac{2\,B\,\tau^2\,v_0\,\alpha^4 + 2\,\tau^2\,v_0\,\alpha\,\beta_\tau + {\beta_\eta}^2}{2\,A\,\tau^2\,v_0\,\alpha^2}, \tag{20}$$

$$\psi^{-3}\ \&\ \xi^1 \text{ with } \psi^0\ \&\ \xi^2\text{:}\ \ \alpha = \alpha(\tau) \qquad \text{only.} \tag{21}$$

Then, the coefficients of ψ^{-3}, ψ^{-2} and ψ^{-1} give rise to the same equation,

$$2\,\eta\,\tau\,v_0\,\alpha(\tau) + 2\,\eta\,\tau^2\,v_0\,\alpha'(\tau) + \beta_\eta(\eta,\tau) + \eta\,\beta_{\eta\eta}(\eta,\tau) = 0, \tag{22}$$

which is solved out symbolically as

$$\beta(\eta,\tau) = -\frac{\eta^2\,\tau\,v_0\,\alpha}{2} + \beta_0(\tau), \tag{23}$$

where the prime sign denotes the first derivative with respect to τ, $\beta_0(\tau)$ is a differentiable function but α reduces to a constant. With the relevant expressions combined together, we arrive at a family of *exact analytic nebulon solutions* to equation (5), as follows,

$$\Phi(\xi,\eta,\tau) = \frac{3\,B\,\alpha^2}{A}\,\mathrm{Sech}^2\left[\frac{\eta^2\,\alpha\,\tau\,v_0}{4} - \frac{\alpha\,\xi}{2} - \frac{\beta_0(\tau)}{2}\right] - \frac{\beta_0'(\tau)}{A\,\alpha} - \frac{B\,\alpha^2}{A}. \tag{24}$$

The nebulon structures will be discussed next.

5 Discussions and conclusions

The nebulon structures via solution (24) are solitonic, with the exact solitary wave solution in reference [12] (Eq. (9) therein) as its special case, with $\alpha = -\sqrt{U_0/B}$ and $\beta_0(\tau) = -U_0\,\alpha\,\tau$. As seen below, solution (24) can go beyond the normal solitary waves.

The nebulon structures via solution (24) (including its amplitude and velocity) and auto-Bäcklund transformation via equations (7) and (9–15) can be determined by the parameters, A, B and v_0, of the dusty plasma system under investigation. The nebulon structures also rely on the initial conditions through α and $\beta_0(\tau)$.

In Figures 2–6, (A) the coordinates (ξ,η,τ) for solution (24) have been transformed back to the aforementioned spherical coordinates (r,θ,t) with the understanding of the axle symmetry and normalization, and correspondingly, to the Cartesian coordinates (x,y,z,t), normalized as well, with the axle symmetry about the z-axis; and (B) the values chosen for the parameters and functions occurring in solution (24) are purely for the purpose of picture drawing and qualitative analysis. In reality,

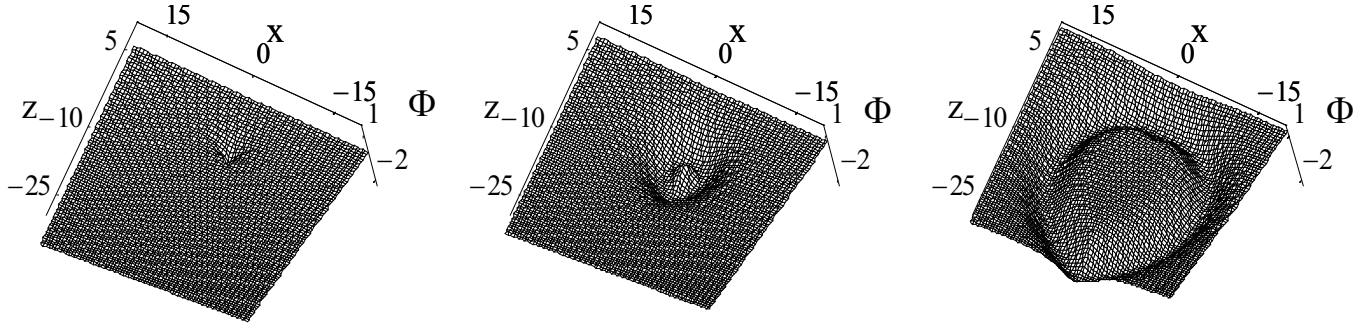

Fig. 2. Observable nebulon surface via solution (24) of equation (5), for the electrostatic potential Φ in a space or laboratory un-magnetized dusty plasma, with the parameters and functions chosen as $\epsilon = 0.01$, $\sigma_i = 0.4$, $\alpha = 5$, $\mu = 1.5$, $v_0/\mid v_0 \mid = 1$ and $\beta_0(t) = (1/50)\sin(4\,t/5)$. The values of time used for the three cartoon graphs are $t = -5$, 2 and 9 respectively. Note that we look up from the bottom.

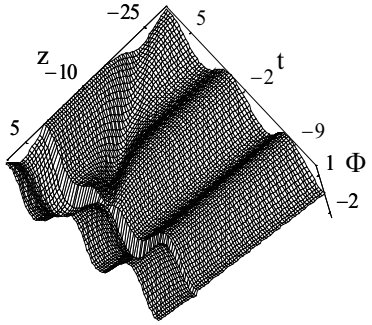

Fig. 3. Observable time evolution of the nebulon verses the axis z. Everything is the same as Figure 2 except that $x = 0$ but t varies.

the detailed application of the nebulon structures requires a thoughtful choice of those parameters and functions.

Figure 2 is a set of animation graphs showing the birth and expansion of a nebulon via expression (24). Each graph, or each "photo" taken at a designated time, gives rise to the sectional drawing of the nebulon, or the watermelon-rind-like or Earth-crust-like solitonic structure "cutting" in the middle, so as to describe the electrostatic potential in a space or laboratory un-magnetized dusty plasma. By virtue of the axle symmetry, we can use such sectional drawing to represent the whole rind or crust. However, as time goes on and as seen in Figure 2 (and other figures next), the spherical shape of the rind or crust deforms because of the latitude dependence of the phase velocity of the nebulon, and the ambient field fluctuates because of the existence of $\beta_0(\tau)$ function.

From Figure 2 (and other figures next), we understand that a nebulon structure with certain constant amplitude but varying $\beta_0(\tau)$ can exist when the latitude perturbation is considered, which is more general than the claim in reference [12], and different from the report by references [11,28] on the non-existence of an exact analytic solution (without the latitude perturbation there).

Figures 3 and 4 depict the time evolution around the birth of a nebulon structure for Figure 2 verses the z-axis, with Figure 4 also indicating both the further solitonic expansion of the nebulon and long-time history before the birth of the nebulon. In Figures 3 and 4, by setting $x = 0$, we investigate the electrostatic potential field along the z-axis, and looking towards both the north and south poles, we discover a single soliton on each side moving away from us. The speeds of those solitons are different since there is no latitude symmetry. The ambient-field fluctuations are clear in Figures 3 and 4. The two solitons are the dark/rarefactive solitons since this plasma system lead to this type of solitons only [29].

Figure 5 provides us with the time evolution of another nebulon structure. The form of $\beta_0(t)$ assumed here is different from that for Figure 3, but the birth and expansion of the nebulon aboard the ambient field are similar to those in Figure 3.

Some nebulons can expand in space, as displayed in Figures 2–5, while other nebulons can shrink, as revealed in the set of animation graphs of Figure 6, depending on the choices of the parameters and functions of solution (24). However, different from that reported in reference [12] (the lines below Eq. (4) and above Eq. (10) there), we see that v_0 is not the only decisive factor for a nebulon to propogate outwards or inwards. Even if with the same v_0 chosen, the expanding nebulon in Figure 2 and shrinking nebulon in Figure 6 can both exist. The reason is the different selection of $\beta_0(t)$'s.

We note that the nonstationary lump-pulse profile numerically obtained in reference [12] (i.e., Figs. 1–3 there) seems a part belonging to the nebulon evolution history presented in this paper, since that profile looks like the first graph of Figure 2, the thick solid line in Figure 4, as well as the birth period of a nebulon shown in Figures 3 and 5.

The nebulon structures revealed in Figures 2–6 can be treated as a set of the *(3+1)-dimensional, possibly observable effects*, which may help to understand the salient features of multi-dimensional dust acoustic waves in the space and laboratory un-magnetized dusty plasmas. Hopefully the future space/laboratory plasma experiments could investigate those effects.

In conclusion, space and laboratory dusty plasma physics are among the most active frontiers, since plasmas and dust are a couple of the omnipresent constituents of the Universe. The nonlinear dust-acoustic-wave

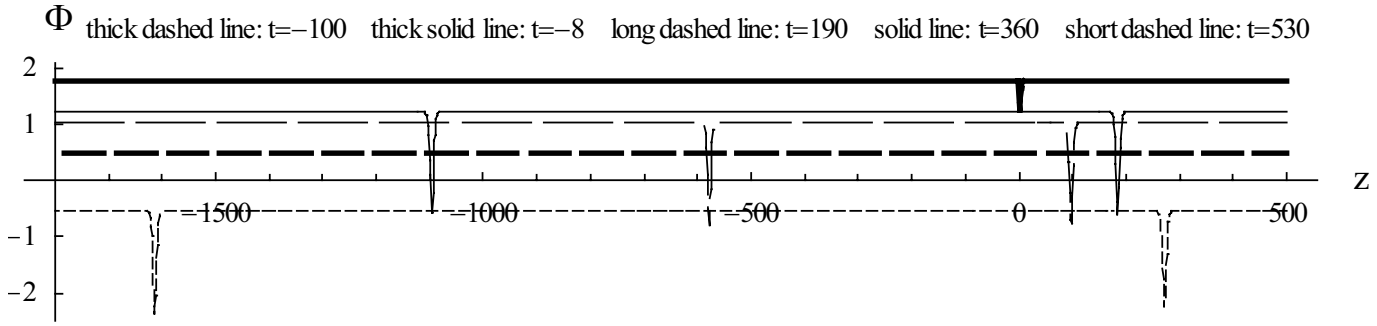

Fig. 4. Specific photographs taken for Figure 3, at different times.

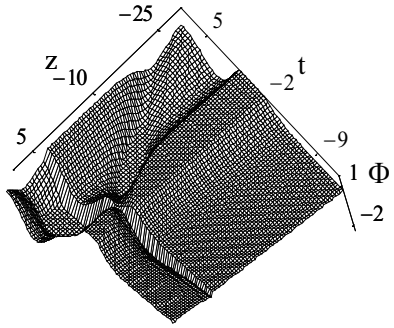

Fig. 5. Another view on the time evolution of the nebulon verses the axis z. Everything is the same as Figure 3 except that $\beta_0(t) = (1/10)\, e^{-(t-2)^2/10}$.

propagation in a space or laboratory un-magnetized dusty plasma is hereby considered with computerized symbolic computation, which is described by equation (5). What we have obtained is an auto-Bäcklund transformation and the analytically-expressed spherical nebulons for the electrostatic potential in such a plasma. With the above figures, we have discussed some salient features of the nebulon structures, and proposed the relevant, (3+1)-dimensional, possibly-observable nebulonic effects for the future space and laboratory plasma experiments.

We express our sincere thanks to the referees and Academician C.-H. Lee for their valuable comments. This work has been supported by the Excellent Young Teachers Program of the Ministry of Education of China, by the National Natural Science Foundation of China under Grants No. 10272017 and No. 60372095, by the National Key Basic Research Special Foundation (NKBRSF) of China under Grant No. G1999032701, by the W.T. Wu Foundation on Mathematics Mechanization, by the Talent Construction Special Fund of Beijing University of Aeronautics and Astronautics, by the Discipline Construction Grant BHB985-1-7 of Beijing University of Aeronautics and Astronautics under the Action Plan for the Revitalization of Education in the 21st Century of the Ministry of Education of China. BT also thanks the Enterprise Chair Professors Programme of Beijing University of Posts and Telecommunications and the Bright Oceans Corporation. YTG would like to acknowledge the Cheung Kong Scholars Programme of the Ministry of Education of China and Li Ka Shing Foundation of Hong Kong.

References

1. L.H. Aller, Nebula, in *Collier's Encyclopedia* (Macmillan Edu. Co., New York & Collier Macmillan Canada, Inc., Toronto, 1991), Vol. 17, p. 270; Anonymous Author, Nebula, in *the New Encyclopedia Britannica* (Encyclopedia Britannica, Inc., Chicago/London, 1998, Int. Chinese Ed., Encyclopedia of China Publishing House, Beijing, 1999), Vol. 12, p. 47
2. H. Bond et al., Hubble Heritage Team (STScI/AURA), NASA. Photograph posted at `http://antwrp.gsfc.nasa.gov/apod/image`
3. D. Gurnett, E. Grun, D. Gallagher, W. Kurth, F. Scarf, Icarus **53**, 236 (1983); D. Tsintikidis, D. Gurnett, W.

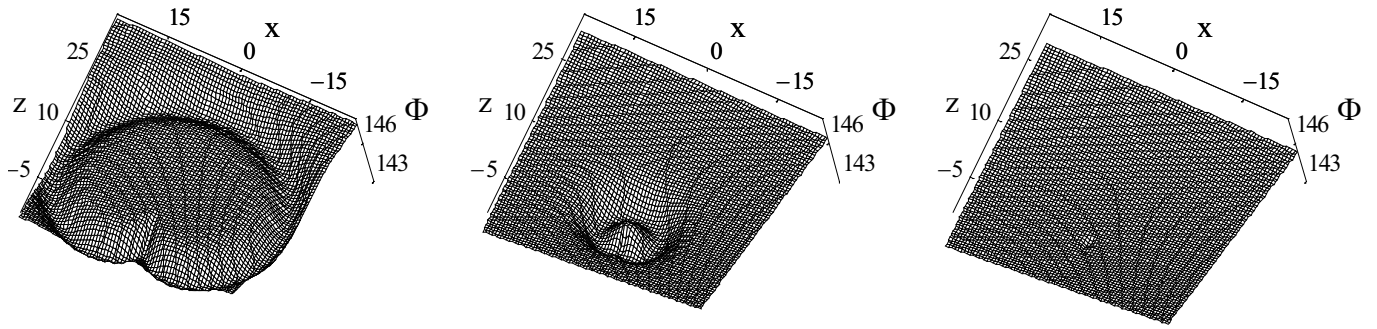

Fig. 6. One more set of cartoon graphs on the observable nebulon surface Φ. Everything is the same as Figure 2 except that $\beta_0(t) = 2\,t + \frac{1}{50}\sin(4\,t/5)$, and that $t = -8$, -2 and 4 respectively.

Kurth, L. Granroth, Geophys. Res. Lett. **23**, 997 (1996); D. Gurnett, J. Ansher, W. Kurth, L. Granroth, Geophys. Res. Lett. **24**, 3125 (1997); M. Horanyi, Phys. Plasmas **7**, 3847 (2000)
4. D.A. Mendis, Plasma Sources Sci. Technol. **11**, A219 (2002)
5. N.N. Rao, P.K. Shukla, M.Y. Yu, Planet. Space Sci. **38**, 543 (1990)
6. A. Barkan, R.L. Merlino, N. D'Angelo, Phys. Plasmas **2**, 3563 (1995); N. D'Angelo, J. Phys. D **28**, 1009 (1995)
7. D.A. Mendis, M. Rosenberg, Ann. Rev. Astron. Astrophys. **32**, 418 (1994)
8. C.K. Goertz, Rev. Geophys. **27**, 271 (1989)
9. P.K. Shukla, A.A. Mamun, *Introduction to Dusty Plasma Physics* (Institute of Physics Publishing, Bristol, 2001)
10. J.X. Ma, J. Liu, Phys. Plasmas **4**, 253 (1997); A.A. Mamun, Astrophys. Space Sci. **268**, 443 (1999)
11. A.A. Mamun, P. Shukla, Phys. Lett. A **290**, 173 (2001)
12. J.K. Xue, Phys. Lett. A **314**, 479 (2003)
13. J.R. Franz, P.M. Kintner, J.S. Pickett, Geophys. Res. Lett. **25**, 1277 (1998); R. Ergun, C. Carlson, J. McFadden, F. Mozer, G. Delory, W. Peria, C. Chaston, M. Temerin, I. Roth, L. Muschietti, R. Elphic, R. Strangeway, R. Pfaff, C. Cattell, D. Klumpar, E. Shelley, W. Peterson, E. Moebius, L. Kistler, Geophys. Res. Lett. **25**, 2041 (1998)
14. S. Maxon, J. Viecelli, Phys. Rev. Lett. **32**, 4 (1974); Phys. Fluids **17**, 1674 (1974); Y. Hase, S. Watanabe, H. Tanaca, J. Phys. Soc. Jpn **54**, 4115 (1985); S.K. El-Labany, S.A. El-Warraki, W.M. Moslem, J. Plasma Phys. **63**, 343 (2000)
15. M. Coffey, Phys. Rev. B **54**, 1279 (1996); B. Tian, Y.T. Gao, Comput. Math. Appl. **31**, 115 (1996); Y.T. Gao, B. Tian, Acta Mech. **128**, 137 (1998); B. Tian, Int. J. Mod. Phys. C **10**, 1089 (1999); W.P. Hong, Y. Jung, Phys. Lett. A **257**, 149 (1999)
16. G. Das, J. Sarma, Phys. Plasmas **6**, 4394 (1999)
17. B. Tian, W. Li, Y.T. Gao, Acta Mech. **160**, 235 (2003)
18. W.P. Hong, Y. Jung, Z. Naturforsch. A **54**, 549 (1999); W.P. Hong, M. Yoon, Z. Naturforsch. A **56**, 366 (2001); R. Ibrahim, Chaos, Solitons & Fractals **16**, 675 (2003); R. Ibrahim, IMA J. Appl. Math. **68**, 523 (2003)
19. M.P. Barnett, J.F. Capitani, J. Von Zur Gathen, J. Gerhard, Int. J. Quant. Chem. **100**, 80 (2004)
20. B. Tian, Y.T. Gao, Eur. Phys. J. B **42**, 441 (2004)
21. Z.Y. Yan, H.Q. Zhang, J. Phys. A **34**, 1785 (2001); Sirendaoreji, J. Phys. A **32**, 6897 (1999); W.P. Hong, S.H. Park, Int. J. Mod. Phys. C **15**, 363 (2004); F.D. Xie, X.S. Gao, Comm. Theor. Phys. **41**, 353 (2004); B. Li, Y. Chen, H.N. Xuan, H.Q. Zhang, Appl. Math. Comput. **152**, 581 (2004); Y.T. Gao, B. Tian, Phys. Plasmas **10**, 4306 (2003); Nuovo Cim. B **118**, 175 (2003); Comput. Math. Appl. **45**, 731 (2003)
22. Y.T. Gao, B. Tian, Int. J. Mod. Phys. C **12**, 1357 (2001)
23. Y.T. Gao, B. Tian, Int. J. Mod. Phys. C **12**, 879 (2001)
24. Y.T. Gao, B. Tian, Phys. Lett. A **301**, 74 (2002)
25. Y.T. Gao, B. Tian, Phys. Plasmas **8**, 67 (2001)
26. Y.T. Gao, B. Tian, Nuovo Cim. B **116**, 119 (2001)
27. D. Zwillinger, *Handbook of Differential Equations* (Academic Press, Boston, 1989)
28. A.A. Mamun, P. Shukla, Phys. Plasmas **9**, 1468 (2002)
29. B. Tian, Y.T. Gao, Phys. Lett. A (2005, in press, No. PLA14316)